

## Laboratory Testing of Embankment on Soft Soil by Shaking Table

Ripon Hore, PhD<sup>1</sup>, Sudipta Chakraborty<sup>2</sup>, and Mehedi A. Ansary, PhD<sup>3</sup>

<sup>1</sup> Senior Assistant Engineer, LGED, Bangladesh

<sup>2</sup> Masters Student, Kongju National University, South Korea

<sup>3</sup> Professor, BUET, Bangladesh

E-mail: riponhore@gmail.com

### Abstract

This paper presents the results of shaking table tests on geotextile-reinforced embankment lying on soft clay. Construction of model embankment in a laminar box mounted on a shaking table, instrumentation and results from the shaking table tests have been discussed in detail. The base motion parameters have been varied in different model tests. It is observed from these tests that the response of the embankment with soft clay has been significantly affected by the base acceleration levels, frequency of shaking and magnitude of surcharge pressure on the crest. The effects of these different parameters on acceleration response at different elevations of the embankment, pore pressures and face deformations have also been presented. The results obtained from this study are helpful in understanding the relative performance of reinforced soil-embankment under different test conditions used in the experiments.

**Keywords:** Shaking table, Laminar box, Soft soil, Amplification

### 1. Introduction

The soil-foundation softening may cause damage to the embankment. Today, there is no absolute conclusion on whether the softening effect of cohesive or clayey soils under earthquake excitation should be considered and under what shake condition the damage induced by excess pore water pressure may not be considered in analysis. The soil-foundation composed of clayey soil has become the focus of earthquake engineering in more cases. However, it is rather scarce to study the characteristic of pore water pressure in such soil-foundations with cohesive or clayey soil under earthquake action due to its clay content is thought of relatively high. Although such soil-foundations of higher clay content are not easily susceptible to liquidity, a rise of excess pore water pressure triggered by earthquakes and a drop of effective stress may lead to the soil softening. Based on shaking table tests, this paper attempts to investigate the changing characteristics of the amplification, displacement and pore water pressure in soft soil-foundations under harmonic wave. To simulate actual soil-foundation, the soil and structure interaction (SSI) system has been considered in this experimental study. The soil-foundation in the test has been built with soft soils in Dhaka clay. The physical mechanism responsible for variation behaviour of the pore water pressure in the repeated process has been studied. The results of experimental investigation have been expected to provide some research basis for softening problems of clayey embankment under earthquake actions.

Research in Earthquake Geotechnical Engineering has found considerable development in the recent past. Developments of model testing in earthquake geotechnical engineering, two



aspects of model testing are given importance, namely manual shaking table and laminar box. Design, development, calibration and performance of these equipment are very important (Prasad S. K. et al., 2004). Model testing is the essential requirement of earthquake geotechnical engineering that helps in understanding the behavior of geotechnical facilities and their performance during earthquake. Manual shaking table developed very economically can be used as an alternative to a more sophisticated shaking table. On the other hand, Laminar box is a sophisticated container which can enhance the accuracy in assessing the ground behavior. Laminar box can be used both under normal gravitational and centrifuge environments. Laminar box included sophisticated bearings resulting in near friction less movement between layers and flexible side walls which provided pure shear condition (Prasad S. K. et al., 2004). Latha M. G. et al (2006) has presented Shaking table studies which have been carried out on wrap-faced reinforced soil retaining walls to gain insight into their behaviour under dynamic loads. Model retaining walls have been tested with variations in the acceleration and frequency of base sinusoidal shaking and surcharge loading. It has been observed that the response of wrap-faced geotextile reinforced model soil retaining walls has been significantly affected by the changes in frequency, surcharge and acceleration of base shaking. Acceleration response gets attenuated with increase in surcharge pressure, the difference being more at higher elevations. Increase in surcharge loading or frequency of shaking results in decrease in deformations along the facing. Displacement profile for the facing of the retaining walls has been observed to flatten for higher base accelerations. Horizontal pressures inside the retaining wall are sensitive to frequency of shaking as well as base accelerations. In spite of the limitations associated with small-scale tests, the results from this study provide useful guidelines regarding the relative performance of reinforced soil retaining walls under various test conditions with clear implications for design.

Srilatha N. (2013) has described the effect of frequency of base shaking on the dynamic response of unreinforced and reinforced soil slopes through a series of shaking table tests. Slopes were constructed using clayey sand and geo-grids were used for reinforcing the slopes. Two different slope angles  $45^\circ$  and  $60^\circ$  were used in tests and the quantity and location of reinforcement has been varied in different tests. Acceleration of shaking is kept constant as 0.3 g in all the tests to maximize the response and the frequency of shaking was 2 Hz, 5 Hz and 7 Hz in different tests. The slope has been instrumented with ultrasonic displacement sensors and accelerometers at different elevations. The response of different slopes has been compared in terms of the deformation of the slope and acceleration amplifications measured at different elevations. It is observed that the displacements at all elevations increased with increase in frequency for all slopes, whereas the effect of frequency on acceleration amplifications is not significant for reinforced slopes. Results showed that the acceleration and displacement response is not increasing proportionately with the increase in the frequency, suggesting that the role of frequency in the seismic response is very important. Reinforced slopes showed lesser displacements compared to unreinforced slopes at all frequency levels.

Fleming B. et al(2016) has conducted a new phenomenon to determine the effects of soil improvement on the seismic resistance of piles in soft clay. For the field experiment, a soft soil site in Miami, Oklahoma, was chosen. The test site consisted of a 4.4 m layer of soft clay



overlying a 2.0 m layer of sandy gravel and limestone bed rock. All these papers based on soil of different countries. In this shake table investigation based on Dhaka soft clayey soil. The effect of frequency, amplitude, surcharge, pore water pressure and displacement along the different elevations has been observed.

## 2. Shaking table tests

Model tests are essential when the prototype behavior is complex and difficult to understand. In model testing, usually the boundary conditions of a prototype problem have been reproduced in a small-scale model. Model tests have been used to understand the effects of different parameters and the process leading to failure of prototype at a real time. The model tests can be divided into two categories, namely, those performed under gravitational field of earth (generally called shaking table tests) and those performed under higher gravitational field (centrifuge tests).

### 2.1. Shaking table

In the present study, a computer-controlled servo-hydraulic single degree of freedom (horizontal) shaking table facility has been used to simulate the horizontal shaking action, associated with seismic and other vibration conditions. The shaking table comprises a loading platform of 2 m x 2 m size and payload capacity of 1 t. Shaking has been provided by a digitally controlled servo-hydraulic actuator with  $\pm 200$  mm stroke and 30 kN force rating. A dedicated control room housing the control system includes a host computer to facilitate testing under both constant amplitude and pseudo-random conditions. The shaking table can be operated over an acceleration range of 0.05g to 2g and frequency range 0.05 to 50 Hz with a maximum amplitude of  $\pm 200$  mm. Maximum velocities are 0.3 m/s.



Figure 1: Shake table test apparatus

### 2.2. Laminar box

The major problems associated with laboratory model studies are scaling and boundary effects, especially in studies related to earthquake engineering. In this study, embankment with soft



clay soil models have been constructed in a laminar box to reduce boundary effects as far as practicable. A laminar box is a large shear box consisting of several Frictionless horizontal layers. The laminar box used for the tests is rectangular in cross-section, with inside dimensions 915 mm x 1220 mm x 1220 mm deep, with 20 rectangular hollow aluminum layers, machined so that the friction between layers is minimal. The gap between the successive layers is 2 mm, and the bottom most layer is rigidly connected to the solid aluminum baseplate of size 915 mm x 1220 mm in plan and 15 mm thickness. The layers are separated by linear roller bearings arranged to permit relative movement between the layers in the longitudinal direction with minimum friction. Figure 2 shows the laminar box mounted on the shaking table.



Figure 2. Laminar box mounted on shaking table

## 2.2.1. Description of laminar box:

### 2.2.1.1 The layers

Each layer is a rectangular frame with  $1.22 \times 0.92 \times 0.05 \text{ m}^3$  internal dimension which has been made from the hollow aluminum profiles with  $50 \times 50 \text{ mm}^2$  section and 1.5 mm thickness. The whole system is composed of 24 layers each being set directly on the other making the total height of 1.22 m. In order to minimize the friction between the layers, transfer ball bearings have been used so that the two dimensional motion in the horizontal plane is possible. This ball bearing consists of one main ball having the diameter of 12 mm which has been put in a hemispherical space full of fine balls. These balls are designed in a way that they can be simply and without additional devices installed on the surface of the layer and the base be alighted on the lower wall of the hollow aluminum profile.

### 2.2.1.2 Base plate and saturation and drainage systems

The lowest layer has been fixed on a steel base which this base in its turn, is fixed on a steel plate with same dimension of laminar layers. In addition to preserving the upper layers, the base has some closed space for watering and dewatering via four valves. The water entrance area to the model is covered with porous stone. In this way, not only saturation and drainage of the samples is facilitated but also the bottom of the container gets rather tough, improving the contact of the soil with the bottom of the container and makes better shear stress transition to the model.

For hydraulic cut-off system and the protection of the ball bearings, the inside of the container is covered by a 2 mm thick rubber.

## 2.3. Backfill material

Locally available dry sand was used as the backfill material. Figure 3 shows the particle size distribution of the sand. The sand has been classified as poorly graded sand (SP) according to the Unified Soil Classification System. The sand achieved a maximum dry density of 18 kN/m<sup>3</sup> in a vibration test, and the minimum dry density observed in the loosest state is 15 kN/m<sup>3</sup>. The specific gravity of the sand particles is 2.64. 62% relative density of sand has been used.

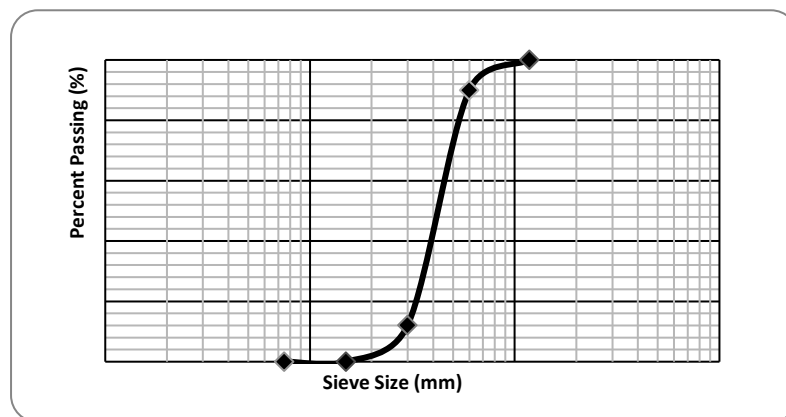


Figure 3: Particle size distribution of test sand

## 2.4. Reinforcement

A non woven polypropylene multifilament geotextile was used for reinforcing the sand in the tests. The individual multifilament are woven together so as to provide dimensional stability relative to each other. The properties of the geotextile are given in Table 1.

Table 1: Geotextile properties

Details	DF 50
1. Reinforcement type	mechanically bonded needle punched
2. Yarn material (staple Fibre)	Polypropylene
3. Mass/unit area (gsm)	322
4. Aperture Size , O <sub>95</sub> (μm)	130
5. Thickness (mm)	2.54
6. Ultimate Tensile Strength (KN/m)	15.5
Ultimate Tensile Strength at 2% strain (KN/m)	15.97
Ultimate Tensile Strength at 5% strain (KN/m)	16.57

## 3. MODEL CONSTRUCTION AND TESTING PROCEDURE

### 3.1 Re constitute clay soil sample:

In this research work Dhaka soft clay soil has been used. The liquid limit of this soil has been found 40%. The water content of this soil sample has been found 23%. For preparing the soil



sample used 50% of water content (1.25 times of liquid limit). From the direct shear test cohesion and friction have been found  $14.8 \text{ KN/m}^2$  and  $10.03$  respectively. After loading had been done, the water content of soil sample was 15% and unconfined compression strength ( $q_u$ ) was 20 kPa. The constitute clay layer thickness of the soil sample is 18". Preparation of re constitute sample has been shown as figure 4. Hydrometer analysis of clay soil has been shown in figure 5. Two pore water pressure sensor: one is base level of sample and another is 18" above the base level have been used in this soil sample. Two acceleration sensor have been placed in the soil sample. After studying XRD data from chemical analysis it has been concluded that Dhaka clay have kaolinite 75 percent and illite 25. After studying XRF analysis of Dhaka soil,  $\text{SiO}_2$  component is 68.77%,  $\text{Al}_2\text{O}_3$  is 15.19% and  $\text{Fe}_2\text{O}_3$  is 9.82%.



Figure 4: Soil Sample preparation

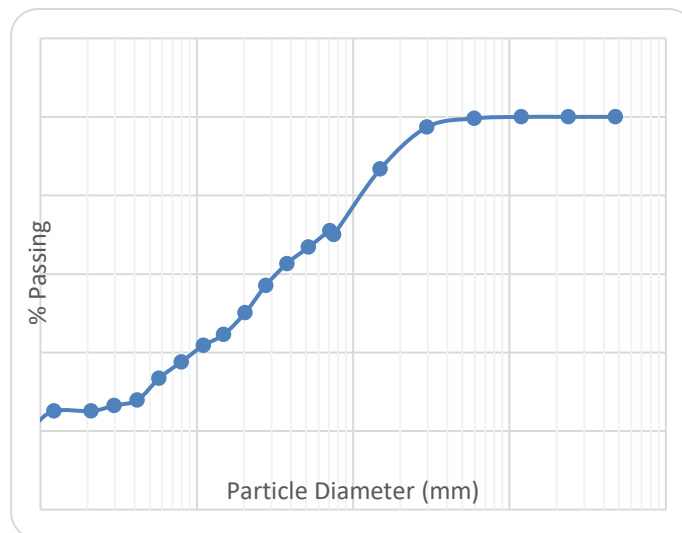


Figure 5: Hydrometer analysis of clay soil

### 3.2 Pluviator:

There are many methods of compaction of soil layers such as tamping, vibration and different types of pluviation (air/water/vacuum). Many researchers gave their efforts in the past on developing methods to control uniformity (Fretti et al. 1995, Zhao et al. 2006, Choi et al. 2009)



and to achieve desired relative density (RD) of sand specimen (Muir and Toki 1982, Rad and Tumey 1987, Lo Presti et al. 1993, Choi et al. 2009, Dave and Dasaka 2012, Srinivasan 2015 et al., Gade 2016 et al.). Among all of these techniques, air pluviation method is broadly used because of its advantage to reconstitute uniform sand bed for laboratory testing. In case of the repeatability and reproducibility of the test results, it is significant to reconstitute the soil sample of desired density.

### 3.3 Testing Process:

The model embankment has been constructed in a laminar box to a size of 915 mm x 1220 mm in plan area and 1220 mm deep. The model was constructed in lifts of equal Height while reinforcing each lift with a layer of woven geotextile. Each geotextile layer has been wrapped at the facing for a length of 150 mm. To achieve uniform density, sand was placed in the laminar box using the pluviation (raining) technique. The height of fall to achieve the desired relative density has been determined by performing a series of trials with different heights of fall. However, the actual relative densities achieved in each test were monitored by collecting samples in small cups of known volume placed at different locations and levels during preparation of the model embankment. After the completion of all lifts up to full height of the wall (406 mm), surcharge in the form of three type concrete slabs (19/34/49 kg)), was applied to anchor the top wrapped geotextile. The facing formwork was removed carefully in sequential lifts from bottom to top after the backfill layers (50 mm) and surcharge have been completed. Figure 6 shows the finished embankment for four-layer with 610 mm clay layer. A typical model configuration showing the instrumentation for the test wall with four layers of reinforcement has been shown in Figure 6. Accelerometers (A) and pressure transducers (P) were embedded in the soil while filling clay/sand at different levels, as shown in the figure. One accelerometer, A1(ch1) has been fixed to the shaking table to record the base acceleration, and the other three accelerometers, A2 for clay layer, A3, A4, A5 and A6 for sand layer have been placed at elevations of 457, 711, 812, 914 and 1016 mm, respectively, from the base at a constant distance of 304 mm from the facing. Three pressure sensors; P1, P2 and P3 have been placed inside the wall, in contact with the measure horizontal displacement, three displacement sensors (LVDTs), L1, L2 and L3, have been positioned at elevations 812, 914 and 1016 mm, respectively, along the facing for the tests with four-layer configurations. LVDTs have been positioned in place using a T-shaped bracket made up of standard L-sections that has been rigidly connected to the laminar box frame and base as shown in Figure 6. The positions of LVDTs are adjusted slightly to match the layer height in the tests with two- and three-layer configurations. The testing programme has been devised to observe the dynamic response of reinforced soil-embankment models subject to variations in the acceleration and frequency of the sinusoidal base shaking and surcharge loading. The response behavior has been recorded in terms of acceleration and pore water pressure at different elevations and the displacements at facing. Each model wall has been subjected to 20 cycles of sinusoidal motion in the direction of the wall longitudinal axis and the response of various instrumentations was monitored using a data acquisition system.





## 6.1. General

Table 1: Test Parameters

39 | Page



1	ST1	0.1	1	19
2	ST2	0.1	3	19
3	ST3	0.1	5	19
4	ST4	0.1	10	19
5	ST5	0.1	12	19
6	ST6	0.1	15	19
7	ST7	0.2	1	19
8	ST8	0.2	3	19
9	ST9	0.2	5	19
10	ST13	0.3	1	19
11	ST14	0.3	3	19
12	ST19	0.4	1	19
13	ST20	0.4	3	19
14	ST24	0.4	15	19
15	ST25	0.5	1	19
16	ST26	0.5	3	19
17	ST31	0.1	1	34
18	ST32	0.1	3	34
19	ST34	0.1	10	34
20	ST54	0.4	15	34
21	ST61	0.1	1	49
22	ST62	0.1	3	49
23	ST64	0.1	10	49
24	ST66	0.1	15	49
25	ST72	0.2	15	49
26	ST78	0.3	15	49
27	ST84	0.4	15	49
28	ST90	0.5	15	49

## 6.2. Acceleration response

Typical acceleration–time histories of the model test ST9, with 19 kg surcharge, 0.2g base acceleration, 5 Hz frequency of base sinusoidal motion at different elevations have been shown in Figure 8. If  $z$  is the elevation along the wall and  $H$  is the full wall height, it is observed that the acceleration recorded at the four elevations (0.25, 0.5, 0.75 and 1) and one of clay layer are almost equal to the base acceleration value. To simplify the presentation of acceleration response at different elevations of the wall, acceleration amplification is used. Acceleration amplification is the ratio of maximum peak to peak acceleration value in the soil to that of the corresponding value of the base motion. Figures 9 to 14 compare the acceleration amplification profile along the height of the wall for different configurations of wall and base motion after each test of 20 cycles of sinusoidal motion. Here the elevation ( $z$ ) is represented in non-dimensional form after normalizing by the full wall height ( $H$ ). Maximum acceleration amplification has been observed at the top of the wall in all the tests. This observation is in concurrence with the results of physical tests reported by Telekes et al. (1994), Murata et al. (1994) El-Emam and Bathurst (2005) and Krishna et al (2007). Figure 9 shows the acceleration amplifications along the height of the wall for different base accelerations of 0.1, 0.2, 0.3, 0.4 and 0.5g from ST2, ST8, ST14, ST20 and ST26 model tests, respectively, which were conducted at 1 Hz frequency, 19 Kg surcharge. Increasing of acceleration amplifications with



increasing of height. However, within the range of tests conducted, acceleration amplifications at the top of the wall for 0.1, 0.2, 0.3, 0.4 and 0.5g base accelerations are 1.06 to 1.22. Figure 10 shows the two sensor in clay soil sample layer for different base accelerations of 0.1, 0.2, 0.3, 0.4 and 0.5g from ST2, ST8, ST14, ST20 and ST26 model tests, respectively, which were conducted at 1 Hz frequency, 19 Kg surcharge. From the figure, find that acceleration amplitude increase with increasing of normalized elevation. Figure 11 shows the effect of frequency of base motion on the acceleration response along the height of the wall for tests ST1, ST2, ST3, ST4, ST5 and ST6 with frequencies of 1, 3, 5, 10, 12 and 15 Hz. As shown in Table 2, these six tests are conducted with base acceleration of 0.1g and 19 kg surcharge on the test wall. From the figure it is observed that acceleration response against frequency variation is not directly proportional. In fact, accelerations are amplified less for 1, 3 and 5 Hz and more for 10 Hz frequencies compared with that of 15 Hz frequency at all elevations but for 12 Hz frequency slightly different than others. However, accelerations at normalized elevations of 0.25, 0.5, 0.75 and 1 were amplified closer to or slightly less than ( $> 1$ ) the base accelerations for the frequency 1, 3 and 5 Hz. On the other hand accelerations at normalized elevations of 0.25, 0.5, 0.75 and 1 were amplified slightly greater than the base accelerations for the frequency 10, 12 and 15 Hz. The difference in acceleration amplifications for different frequencies increases with increase in wall height, resulting in amplifications of 3.26, 2.26 and 3.14 for 10, 12 and 15 Hz frequency, respectively, at a normalized height of 1, whereas the corresponding values are 2.28, 1.58 and 1.43 at a normalized height of 0.25. On the other hand, the difference in acceleration amplifications for different frequencies slightly decreases with increase in wall height, resulting in amplifications of 0.93, 1.04 and 0.96 for 10, 12 and 15 Hz frequency, respectively, at a normalized height of 1, whereas the corresponding values are 0.94, 1.10 and 1.04 at a normalized height of 0.25. These observations highlight the role of the fundamental (resonance) frequency of the system and the proximity of the base excitation frequency to this resonance frequency (Kramer 1996). Figure 12 shows the two sensor in clay soil sample layer for different frequency of 1, 3, 5, 10, 12 and 15 Hz from ST1, ST2, ST3, ST4, ST5 and ST6 model tests, respectively, which were conducted at 0.1 g base acceleration, 19 Kg surcharge. From the figure, find that acceleration amplitude decrease with increasing of normalized elevation for 1 Hz frequency. On the other hand acceleration amplitude increases with increasing of normalized elevation for others frequency. Acceleration response against different surcharge pressures is presented in Figure 13 from tests ST4, ST34 and ST64 with 19, 34 and 49 Kg surcharge pressures respectively. Accelerations at the top of the wall are high with respect to base acceleration to the surcharge pressures, with amplification values of 1.42, 1.33 and 1.00 for 19, 34 and 49 Kg surcharge pressures respectively. Figure 14 shows the two sensor in clay soil sample layer for different base accelerations of 19, 34 and 49 kg from ST4, ST34 and ST64 model tests, respectively, which were conducted at 10 Hz frequency, 0.1 g base acceleration. From the figure, find that acceleration amplitude increase with increasing of normalized elevation for 19, 34 and 49 kg.



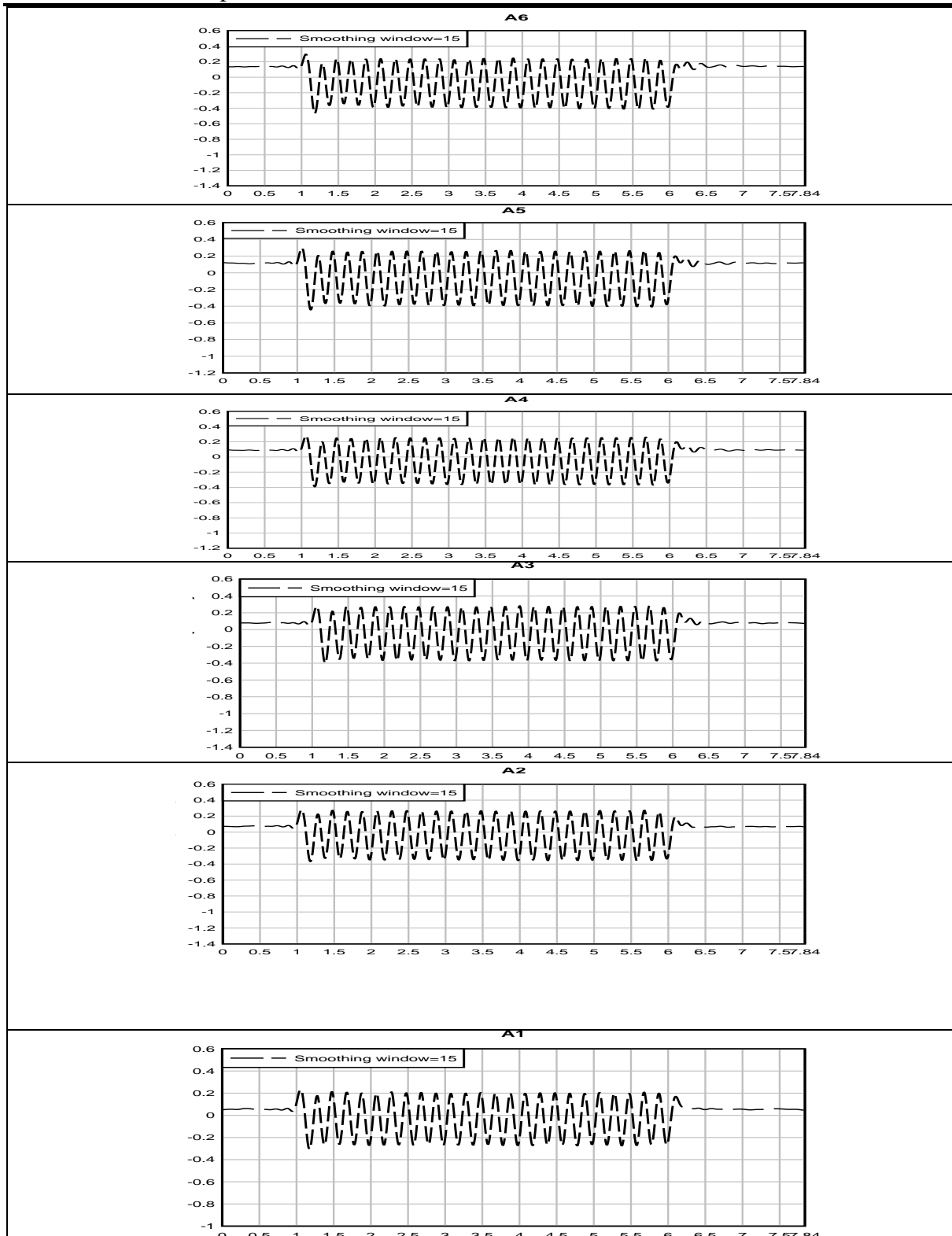


Figure 8: Acceleration histories at different elevations



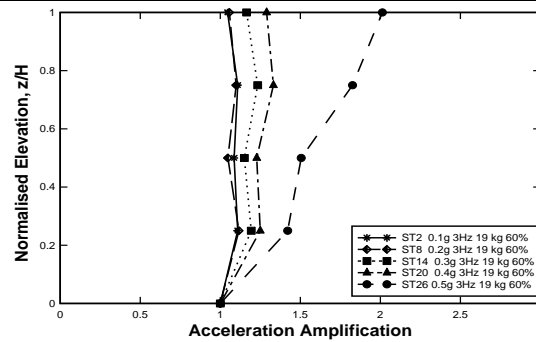


Figure 9: Effect of base acceleration on acceleration amplification

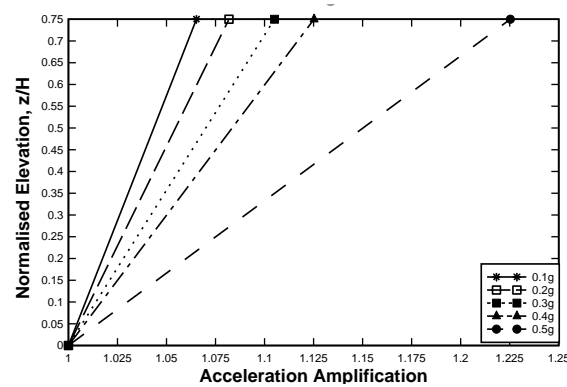


Figure 10: Effect of base acceleration on acceleration amplification (Clay layer)

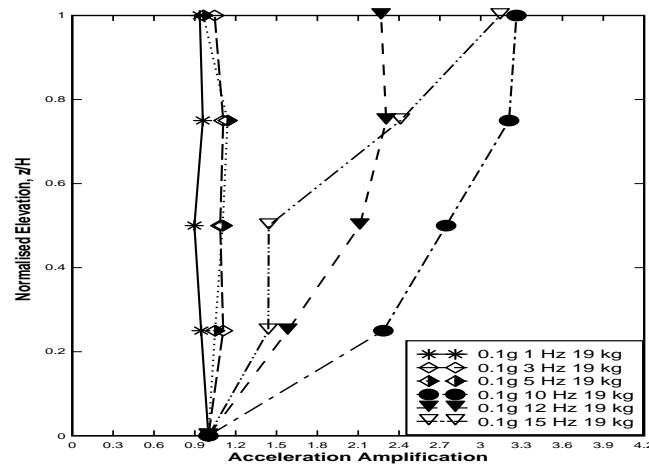


Figure 11: Effect of Frequency on acceleration amplification

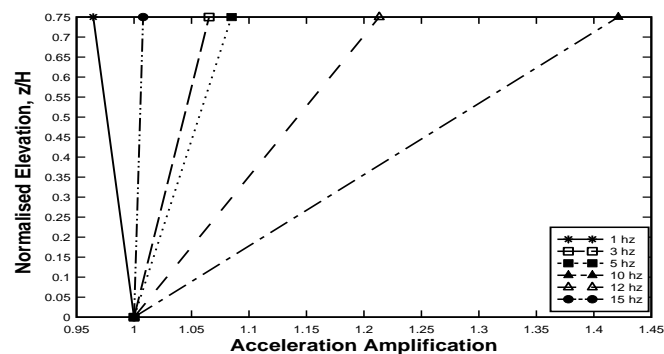


Figure 12: Effect of Frequency on acceleration amplification (clay layer)



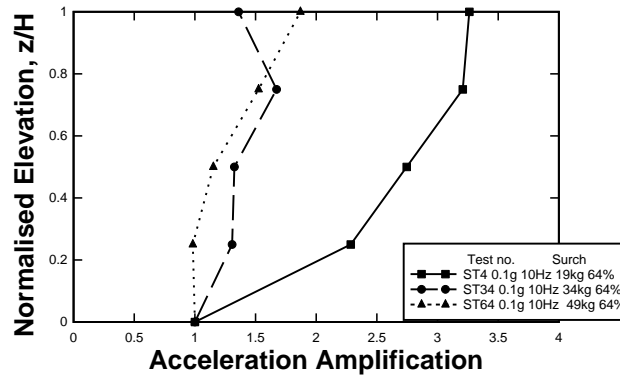


Figure 13: Effect of Surcharge on acceleration amplification

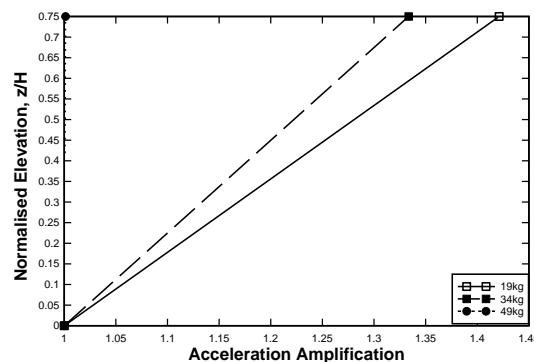


Figure 14: Effect of Surcharge on acceleration amplification (Clay layer)

### 6.3. Face displacement response

Horizontal face displacements along the height of the wall were monitored using three LVDTs positioned as shown in Figure 7. Figures 15 to 17 present the displaced face profiles from various tests after 20 cycles of sinusoidal motion. Here elevation ( $z$ ) and horizontal displacements ( $h$ ) are presented in non-dimensional form after normalizing them by the total height of the wall ( $H$ ). Figure 15 shows the displacement profiles observed for tests ST1, ST2, ST3, ST4, ST5 and ST6 with frequencies 1, 3, 5, 10, 12 and 15 Hz respectively. It is observed that the displacements are highest at highest elevation ( $z/H=0.875$ ). The maximum normalized displacement of 2.01% is observed for 12 Hz frequency; the corresponding values for 1, 3, 5, 10 and 15 Hz frequencies are 0.02, 1.99, 2.00, 2.01 and 1.93%, respectively. Figure 16 presents the displacement profile for tests ST2, ST32 and ST62 after 20 cycles of base motion, providing an insight into the effect of different surcharge loadings of 19, 34 and 49 kg. Displacements at all elevations decreased with an increase in surcharge pressure. From the same figure it can also be observed that the maximum deformation of the wall is 8 mm ( $\delta h/H = 2\%$ ) at a surcharge pressure of 19 kg, whereas it is decreased to 0.2 mm ( $\delta h/H = 0.05\%$ ) at a surcharge pressure of 49 kg. Figure 17 shows normalized displacement profiles of the facing after 20 cycles for different base accelerations of 0.1, 0.2, 0.3, 0.4 and 0.5g from tests ST1, ST7, ST13, ST19 and ST25 respectively. The normalized displacements are relatively high at higher base accelerations. A maximum horizontal displacement of 2.02% of the total wall height,  $H$ , for 0.5g was observed compared with 0.01% for 0.1g base acceleration. The displacements



obtained in the present study are in close agreement with the results presented by Sakaguchi et al. (1992) and Krishna et al (2007) corresponding to the accelerations and frequency levels used in the present study.

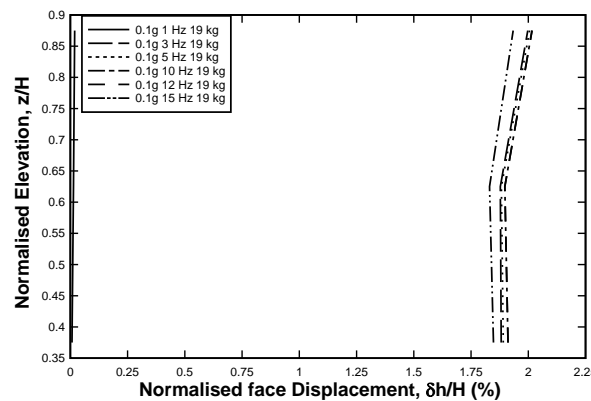


Figure 15: Effect of Frequency on displacement profile

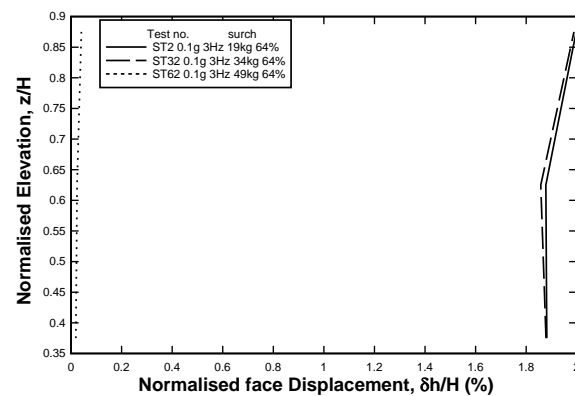


Figure 13:

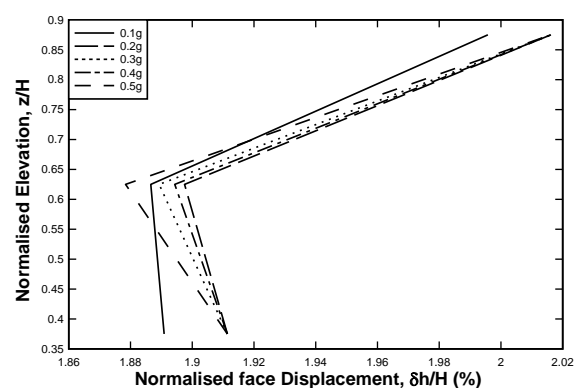


Figure 16: Effect of Surcharge on displacement profile

6.4. Pore Pressure response Figures 18, 19 and 20 present typical pore pressure variations obtained from the model tests. Figure 18 shows variations of the pore pressure from model tests ST66, ST72, ST78, ST84 and ST90 with of base acceleration 0.1, 0.2, 0.3, 0.4 and 0.5 g respectively for 15Hz frequencies and surcharge load 49 kg. From the figure, it is observed that

pore water pressure increase with elevation. The height pore water pressure is 0.38 kPa at base acceleration 0.5g. The highest pore water pressure for model tests ST66, ST72, ST78, ST84 and ST90 is 0.06, 0.09, 0.17, 0.26 and 0.38 kPa respectively. Figure 19 depicts the effect of frequency for a given base acceleration and surcharge on pore water pressures. The pore water pressure variations for tests ST1, ST2, ST3, ST4, ST5 and ST6 with frequency of 1, 3, 5, 10, 12 and 15Hz for 0.1g base accelerations and 19 kg surcharge. It is observed from the figure that pore water pressures increase with increasing elevation. It is also observed that the highest pore water pressure is 0.07 kPa at 10 Hz frequency. The highest pore water pressure for model tests ST1, ST2, ST3, ST4, ST5 and ST6 is 0.02, 0.03, 0.03, 0.11, 0.09 and 0.07kPa respectively. Figure 20 shows variations of the pore pressure from model tests ST24, ST54 and ST84 with of surcharge 19, 34 and 49 kg respectively for 15Hz frequencies and base acceleration 0.4g. From the figure, it is observed that pore water pressure increase with elevation. The height pore water pressure is 0.37 kPa at surcharge load 19 kg. The highest pore water pressure for model tests ST24, ST54 and ST84 is 0.37, 0.33, and 0.26 kPa respectively.

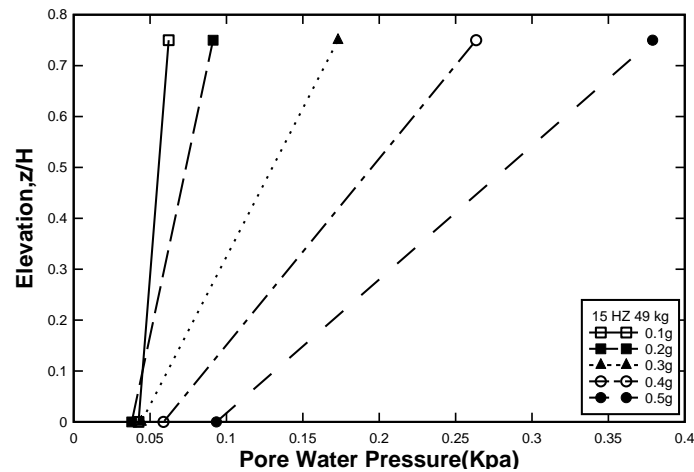


Figure 18: Variations of pore water pressure with respect to Elevation (Effect of base acceleration)

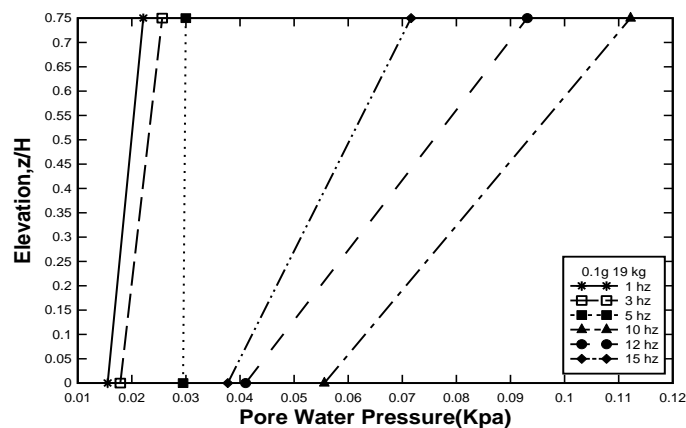


Figure 19: Variations of pore water pressure with respect to Elevation (Effect of Frequency)



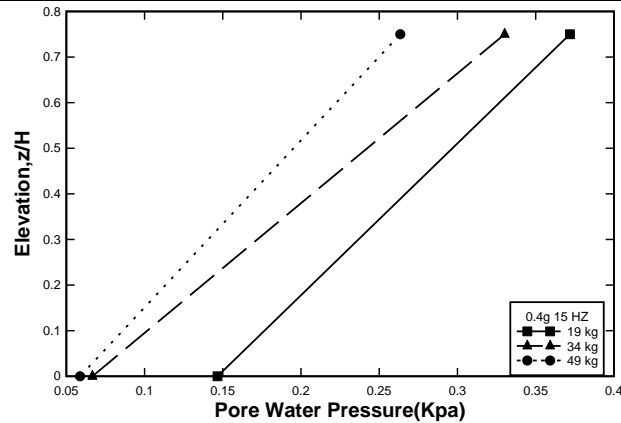


Figure 20: Variations of pore water pressure with respect to Elevation (Effect of Surcharge)

## CONCLUSIONS

The seismic response of geotextile-reinforced embankment with soft clayey soil has been investigated by conducting shaking table tests on model test. A model test with variations in acceleration and frequency of base motion, surcharge pressure on the crest and pore water pressure have been described along with the model preparation, testing methodology and results. It has been observed that the seismic response of the embankment has significantly been affected by the variations base motion, surcharge pressure on the crest and pore water pressure. In general, accelerations have been amplified at higher elevations and with low surcharge pressures. The acceleration amplification response with change in base shaking frequency clearly indicated the role of the fundamental frequency on the response of the system. In some case the face deformations are high for low-frequency shaking, low surcharge pressures and high base accelerations. Pore water pressure is high at higher elevations and with low surcharge pressures high frequency and base acceleration.

## REFERENCES

1. Hebib, S. and Farrell, E.R. (1999). Some Experiences of Stabilizing Irish Organic Soils. Proceeding of Dry Mix Methods for Deep Soil Stabilization (pp. 81-84).
2. M.M. Zumrawi (2014), IACSIT Int. J. Eng. Technol. 6, 439
3. W.R. Day (2001), Soil Testing Manual: Procedures, Classification Data, and Sampling Practices (McGraw-Hill/Education, 2001).
4. S. Haykin (1994), Neural Network: A Comprehensive Foundation (MacMillan College Publishing).
5. T. Fikret Kurnaz,a and Yilmaz Kaya (2019) : Prediction of the California bearing ratio (CBR) of compacted soils by using GMDH-type neural network.
6. Rajasekaran, G., and Rao,S.N. (2000) : Strength characteristics of lime treated marine clay, Proc.Inst.Civ.Engg. Ground Improvement, Vol 4(3)pp.127-136.
7. Dash, S.K., and Hussain, M. (2012) : Lime stabilization of soils: Reappraisal,” Journal of Materials in Civil Engineering, Vol.24, No.6, pp.707-714.
8. Hore, R., Chakraborty, S., Ansary, M. A., Investigation of Model Retaining Wall on Soft Clay, 2022, Web of Scientist: International Scientific Research Journal 3 (02), 402-411.

9. Kamrul, M. K., Hore, R., Forecasting of Rainfall and Temperature Based on the Analysis of Historical data and Future Impact, 2021, Web of Scientist: International Scientific Research Journal 2 (04), 353-372.
10. Akshaya Kumar Sabat (2013): Prediction of California Bearing Ratio of a Soil Stabilized with Lime and Quarry Dust Using Artificial Neural Network .
11. Varghese V, Babu S, Bijuumar R, Cyrus S, Abraham B (2013) Artificial neural networks: a solution to the ambiguity in prediction of engineering properties of fine grained soils. Geotech Geol Eng 31:1187–1205.
12. Chakraborty, S., Hore, R. Ahmed, F., Ansary, M. A., Soft ground improvement at the Rampal Coal Based Power Plant Connecting Road Project in Bangladesh, Geotechnical Engineering Journal of the SEAGS & AGSSEA, AIT December 2017.
13. Hore, R. & Ansary M. A., SPT-CPT Correlations for Reclaimed Areas of Dhaka, Journal of Engineering Science, JES, KUET, June 2018.
14. M. R. Arefin, Hore, R., Ansary, M. A., Development of liquefaction potential map of Dhaka city using SPT test, Journal of Civil Engineering (IEB), 46 (2), 2018, 127-140.
15. Hore, R., M. R. Arefin, Ansary, M. A., Development of Zonation Map Based on Soft Clay for Bangladesh, Journal of Engineering Science 10(1), 2019, 13-18.
16. Hore, R., Chakraborty, S., Ansary, M. A., Field Investigation to Improve Soft Soils Using Prefabricated Vertical Drain, Transportation Infrastructure Geotechnology, September, 2019 (<https://doi.org/10.1007/s40515-019-00093-8>).
17. Hore, R., Chakraborty, S., Shuvon, A. M., Ansary, M. A., Effect of Acceleration on Wrap Faced Reinforced Soil Retaining Wall on Soft Clay by Performing Shaking Table Test, Proceedings of Engineering and Technology Innovation, 2020.
18. Hore, R., Chakraborty, S., Bari, M. F., Shuvon, A. M., Ansary, M. A., Soil Zonation and The Shaking Table Test of The Embankment on Clayey Soil, Geosfera Indonesia, August 2020 (DOI: <https://doi.org/10.19184/geosi.v5i2.17873>)
19. Hore, R., Chakraborty, S., Ansary, M. A., Experimental Investigation of Embankment on Soft Soil Under Cyclic Loading: Effect of Input Surcharges, Journal of Earth Engineering (JEE) Vol. 5, No. 1, (2020).
20. Balasubramaniam, A., Bergado, D., Buensuceso, B. & Yang, W. (1989) Strength and deformation characteristics of limetreated soft clays. Geotechnical Engineering., 20 (1), 49-65.
21. S. Bhatt, P.K. Jain (2014), Am. Int. J. Res. Sci. Technol. Eng. Math. 8, 156 (2014).
22. Fikret Kumaz, T ; Kaya Yilmaz (2019). “Prediction of the California bearing ration (CBR) of compacted soil by using GMDH-type neural network” The European Physical Journal Plus, Volume 134, Issue 7, article id. 326, 15 pp.
23. De Graft-Johnson JWS, Bhatia HS (1969). The engineering characteristics of the lateritic gravels of Ghana. In: Proceedings of 7th international conference on soil mechanics and foundation engineering, vol. 2, Mexico, August 28–29. Bangkok: Asian Institute of Technology; 1969. p. 13–43.
24. Agarwal KB, Ghanekar KD (1970). Prediction of CBR from plasticity characteristics of soil. In: Proceeding of 2nd south-east Asian conference on soil engineering, Singapore, June 11–15, 1970. Bangkok: Asian Institute of Technology; 1970. p. 571–6.



25. Isabel Gonza´lez Farias . William Araujo . Gaby Ruiz (2018) : Properties of Soils Using Parametric and Non-parametric Models, 2018.
26. Ramasubbarao G, Siva G (2013) Predicting soaked CBR value of fine grained soils using index and compaction characteristics. *Jordan J Civ Eng* 7:354–360
27. Patel R, Desai M (2010) CBR predicted by index properties for alluvial soils of South Gujarat. In: *Indian geotechnical conference*, vol 1, pp 79–82
28. Tarun Kumar Rajak, Dr. Sujit Kumar Pal (2015): CBR Values of Soil Mixed with Fly Ash and Lime, 2015
29. Hore, R., Ansary, M. A., Different Soft Soil Improvement Techniques of Dhaka Mass Rapid Transit Project, *Journal of Engineering Science* 11(2), 2020, 37-44. (<https://doi.org/10.3329/jes.v11i2.50896>)
30. Hore, R., Al-Mamun. S., Climate Change and its diverse impact on The Rural Infrastructures in Bangladesh, *Disaster Advances*, Vol. 13 (9) September (2020).
31. Hore, R., Chakraborty, S., Ansary, M. A., “Liquefaction Potential Analysis based on CPT and SPT” *Geotechnical Engineering Journal of the SEAGS & AGSSEA*, December 2020
32. Chakraborty, S., Hore, R., Shuvon, A. M., Ansary, M. A, Dynamic Responses of Reinforced Soil Model Wall on Soft Clay Foundation, *Geotechnical and Geological Engineering*, January 2021. (<https://doi.org/10.1007/s10706-020-01665-z>)
33. Hore, R., Chakraborty, S., Ansary, M. A., Seismic Response of Embankment on Soft Clay Based on Shaking Table Test, *International Journal of Geosynthetics and Ground Engineering*, March 2021. (<https://doi.org/10.1007/s40891-020-00246-7>)
34. Hore, R., Chakraborty, S., Shuvon, A. M., Ansary, M. A., Dynamic Response of Reinforced Soil Retaining Wall Resting on Soft Clay, *Transportation Infrastructure Geotechnology*, February 2021. (<https://doi.org/10.1007/s40515-021-00156-9>).
35. Chakraborty, S., Hore, R., Shuvon, A. M., Ansary, M. A, Physical and numerical analysis of reinforced soil wall on clayey foundation under repetitive loading: effect of fineness modulus of backfill material, *Arabian Journal of Geosciences*, June 2021. (DOI:10.1007/s12517-021-07317-7)
36. Hore, R., Chakraborty, S., Shuvon, A. M., Ansary, M. A., Numerical Verification for Seismic Response of Reinforce Soil Embankment on soft Clay foundation, *Geotechnical Engineering Journal of the SEAGS & AGSSEA*, June 2022.
37. Chakraborty, S., Hore, R., Shuvon, A.M. et al. Effect of Surcharge Pressure on Model Geotextile Wrapped-Face Wall Under Seismic Condition. *Iran J Sci Technol Trans Civ Eng* (June, 2022). <https://doi.org/10.1007/s40996-022-00900-2>
38. Koliass, S, V Kasselouri-Rigopoulou and A Karahalios. (2005) Stabilisation of Clayey Soils with High Calcium Fly Ash and Cement. *Cement and Concrete Composites* 27(2), 301-313.
39. Imoh Christopher Attah, Fidelis Onyebuchi Okafor, Onuegbu Okoronkwo Ugwu (2020) Optimization of California bearing ratio of tropical black clay soil treated with cement kiln dust and metakaolin blend.
40. Mudassir Iqbal, Kennedy C. Onyelowe, Fazal E. Jalal (2021). “Smart computing models of California bearing ratio, unconfined compressive strength, and resistance value of activated ash-modified





- soft clay soil with adaptive neuro-fuzzy inference system and ensemble random forest regression techniques” ,\_Multiscale and Multidisciplinary Modeling, Experiments and Design,
41. Chakraborty, S., Hore, R., Shuvon, A. M., Ansary, M. A., Experimental Investigation of Embankment on Soft Soil under Cyclic Loading: Effect of Input Acceleration, 4th International Conference on Advances in Civil Engineering 2018 (ICACE 2018), 19 –21 December 2018, CUET.
  42. Chakraborty, S., Hore, R., Shuvon, A. M., Ansary, M. A., Development of Zonation for Bangladesh based on Soft Clay Using GIS, 4th International Conference on Advances in Civil Engineering 2018 (ICACE 2018), 19 –21 December 2018, CUET.
  43. Hore, R., Chakraborty, S., Ansary, M. A., Investigation of Model Retaining Wall on Soft Clay, 2022, Web of Scientist: International Scientific Research Journal 3 (02), 402-411.
  44. Kamrul, M. K., Hore, R., Forecasting of Rainfall and Temperature Based on the Analysis of Historical data and Future Impact, 2021, Web of Scientist: International Scientific Research Journal 2 (04), 353-372.
  45. Tarannum, I., Hore, R., Condition Analysis of the Existing Cyclone Shelter of Disaster-Prone Area in Bangladesh, 2021, Web of Scientist: International Scientific Research Journal 2 (04), 380-385.
  46. Hore, H., Probable Liquefaction Problem in Bangladesh, Innovative Technological: Methodical Research Journal, 2(05), 7–25, May 2021.

